A Hybrid Vortex Method for the Simulation of 3D Incompressible Flows

Chloe Mimeau, Georges-Henri Cottet, Iraj Mortazavi

A Hybrid Vortex Method for the simulation of 3D incompressible flows

C. Mimeau[1], G.-H. Cottet[2], and I. Mortazavi[1]

[1] Conservatoire National des Arts et Métiers, M2N Lab EA-7340, Paris, France
chloe.mimeau@cnam.fr
iraj.mortazavi@cnam.fr
[2] Grenoble-Alpes University, LJK Laboratory F-38041, Grenoble, France
georges-henri.cottet@univ-grenoble-alpes.fr

Abstract. A hybrid particle/mesh Vortex Method, called remeshed vortex method, is proposed in this work to simulate three-dimensional incompressible flows. After a validation study of the present method in the context of Direct Numerical Simulations, an anisotropic artificial viscosity model is proposed in this paper in order to handle multi-resolutions simulations in the context of vortex methods.

Keywords: Vortex Method · Semi-Lagrangian · Anisotropic artificial viscosity model.

1 Introduction

Among the numerous numerical approaches used in CFD, Lagrangian methods, also called particle methods, occupy an important place thanks to their intuitive and natural description of the flow as well as their low numerical diffusion and their stability. Indeed, in Lagrangian approaches, the physical quantities involved in the simulated problem are discretized onto a set of particles evolving spatially in the domain according to the problem dynamics. The particles are therefore characterized by their position in the computational domain and the value of the physical quantity they are carrying. Vortex methods [5] belong to this class of Lagrangian approaches and will constitute the key point of the present work. In Vortex methods, the particles discretize the Navier-Stokes equations in their velocity ($\mathbf{u}$) - vorticity ($\boldsymbol{\omega}$) formulation. This formulation allows to directly point to the essence of vorticity dynamics in incompressible flows, which is characterized by advection and diffusion as well as stretching and change of orientation.

However, Vortex methods exhibit difficulties inherent to particle methods and related to the particle distortion phenomenon, which manifests itself by the clustering or spreading of the flow elements in high strain regions, thus implying the loss of convergence of the method. The remeshing technique [8] may be considered as one of the most efficient and popular method to bypass the inherent problem of particle distortion. It consists in periodically redistributing the particles onto an underlying Cartesian grid in order to ensure their overlapping and thus the convergence of the solution. These hybrid Lagrangian/Eulerian

ICCS Camera Ready Version 2019
To cite this paper please use the final published version:
DOI: 10.1007/978-3-030-22747-0_46

approaches are characterized by the fact that the vorticity and the velocity variables are both resolved on the particles field and on a Cartesian grid.

In this work the remeshing procedure is performed in a directional way [9]. This approach transforms the usual tensorial computations (based on 3D-stencils) into 1D advection/remeshing problems in each direction, thus decreasing substantially the comptutational cost of this procedure. As the Cartesian grid used in the present work is uniform and fixed in time, the simulations of flows at high Reynolds numbers involve prohibitive computational efforts. To encouter this problem, we propose in the present paper *bi-level* simulations. The bi-level approach may be considered as a hybrid procedure since it relies on a resolved vorticity field while the related velocity field is filtered. The artificial viscosity model derived here for this purpose is directly based on Vortex Method framework, according to [3].

This paper is organized as follows. We will first describe the remeshed Vortex Method, giving the governing equations and the fractional step algorithm used to discretize them. Then we will expose the artificial viscosity model proposed here to perform bi-level simulations. The last section will be dedicated to the numerical results: both direct numerical simualtions and bi-level simulations will be validated in the context of a Taylor-Green Vortex at $Re = 1600$.

2 Remeshed Vortex Method

2.1 Governing equations

This study is based on the vorticity formulation of the incompressible Navier-Stokes equations, called the Vorticity Transport Equations. In a domain D, these equations read:

$$\frac{\partial \boldsymbol{\omega}}{\partial t} + (\mathbf{u} \cdot \nabla)\boldsymbol{\omega} - (\boldsymbol{\omega} \cdot \nabla)\mathbf{u} = \frac{1}{Re}\Delta\boldsymbol{\omega} \tag{1}$$

$$\Delta\mathbf{u} = -\nabla \times \boldsymbol{\omega}, \tag{2}$$

where $\boldsymbol{\omega}$, $\mathbf{u}$ and Re respectively denote the vorticity, the velocity and the Reynolds number. One can distinguish in Eq. 1 the advection term $(\mathbf{u} \cdot \nabla)\boldsymbol{\omega}$, the stretching term $(\boldsymbol{\omega} \cdot \nabla)\mathbf{u}$ (which vanishes in 2D) and the diffusion term $\Delta\boldsymbol{\omega}/Re$. The Poisson equation 2 is derived from the incompressibility condition $\nabla \cdot \mathbf{u} = 0$ and allows to recover the velocity field $\mathbf{u}$ from the vorticity field $\boldsymbol{\omega}$. This system of equations has to be complemented by appropriate conditions at the boundaries of computational domain D.

2.2 Fractional step algorithm

To solve the vorticity transport equations 1-2, the flow is discretized onto particles that carry the vorticity field $\boldsymbol{\omega}$ transported at the velocity $\mathbf{u}$ and the

ICCS Camera Ready Version 2019
To cite this paper please use the final published version:
DOI: 10.1007/978-3-030-22747-0_46

resolution of the governing equations is based on a splitting algorithm, which consists at each time step in successively solving the following equations:

$$\Delta \mathbf{u} = -\nabla \times \boldsymbol{\omega} \tag{3}$$

$$\frac{\partial \boldsymbol{\omega}}{\partial t} = \boldsymbol{\nabla} \cdot (\boldsymbol{\omega} : \mathbf{u}) \tag{4}$$

$$\frac{\partial \boldsymbol{\omega}}{\partial t} = \frac{1}{Re} \Delta \boldsymbol{\omega} \tag{5}$$

$$\frac{\partial \boldsymbol{\omega}}{\partial t} + (\mathbf{u} \cdot \nabla)\, \boldsymbol{\omega} = 0 \tag{6}$$

$$\Delta t_{adapt} = \frac{\mathrm{LCFL}}{\|\nabla \mathbf{u}\|_\infty} \tag{7}$$

Equation	Time discr. method	Space discr. method
Poisson equation (3)	-	Spectral method
Stretching (4)	RK3 scheme	4^{th} order centered FD
Diffusion (5)	Implicit Euler scheme	Spectral method
Advection (6)	RK2 scheme	$\Lambda_{4,2}$ remeshed vortex method
Adaptive time step (7)	-	4^{th} order centered FD (LCFL < 1)

Table 1: Time and space discretization methods used for the resolution of the viscous splitting algorithm (eqs. 3 to 7).

The discretization of each equation of the fractional step algorithm is realized in this study by using a semi-Lagrangian Vortex method, called the remeshed Vortex method. Table 1 gives the time and space discretization schemes used in this work to solve them. The advection of vorticity field (eq. 6) is performed in a Lagrangian way using a Vortex method. This Lagrangian approach provides a natural and efficient way to solve the non-linear convection term, with low numerical diffusion. Once the particles carrying the vorticity field have been transported, they are redistributed on an underlying Cartesian grid using a remeshing kernel of type $\Lambda_{4,2}$ [4]. The $\Lambda_{p,r}$ remeshing kernels are piecewise polynomial functions of regularity $\mathcal{C}^r$, satisfying the conservation of the first p moments. The $\Lambda_{4,2}$ kernel therefore satisfies the first 4 moments and is of regularity $\mathcal{C}^2$. It contains 6 points in its 1D-support, which means that each particle is redistributed onto 6 points in each direction.

In this work, the particle advection and the remeshing procedure are performed using a directional splitting approach [9]. It consists in solving the advection and remeshing problems direction by direction. As a consequence, if the chosen kernel contains S points in its 1D-support, the number of operations with the directional splitting method compared to the tensorial approach goes from $\mathcal{O}(S^2)$ to $\mathcal{O}(2S)$ in 2D and from $\mathcal{O}(S^3)$ to $\mathcal{O}(3S)$ in 3D (see Fig. 1). If

ICCS Camera Ready Version 2019
To cite this paper please use the final published version:
DOI: 10.1007/978-3-030-22747-0_46

we consider the $\Lambda_{4,2}$ kernel ($S = 6$) used in the present work, the directional splitting method thus allows to divide the number of operations by 12 for each particle. This directional splitting consequently allows for a drastic reduction of the computational cost in terms of regridding operations.

The systematic remeshing of particles onto an Eulerian grid at each time step enables to ensure the overlapping of particles required for the convergence of the method. Moreover the presence of the grid allows to discretize the other equations using efficient and/or fast grid methods (finite differences and spectral method based on FFT evaluations). In the present algorithm, equations 3 to 5 are solved on the grid. Note that the stretching problem 4 is considered here in its conservative formulation, $\partial_t \boldsymbol{\omega} = \boldsymbol{\nabla} \cdot (\boldsymbol{\omega} : \mathbf{u})$.

Finally, the value of the adaptive time step is evaluated (on the grid) at the end of the fractional step algorithm according to the infinite norm of the velocity gradient (cf eq. 7), which provides a more relaxed condition compared to classical CFL conditions. The Lagrangian CFL number, called LCFL, must be taken lower or equal to 1. In this work we set LCFL $= 1/8$.

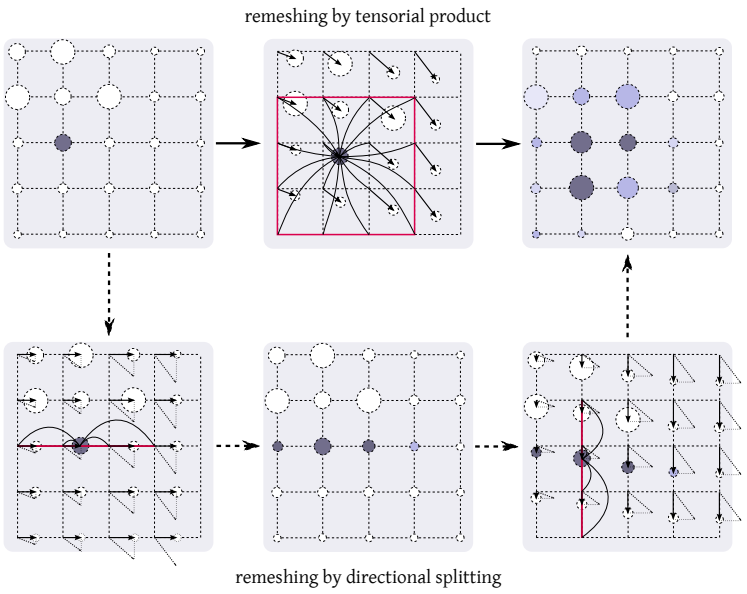

Fig. 1: 2D schematic representation of a remeshing procedure using a tensorial product (on top, depicted by plain arrows) and a directional splitting (on bottom, depicted by dashed arrows). The red lines indicate the support of the remeshing kernel. In this example, the kernel has a 1D-support of 4 points.

ICCS Camera Ready Version 2019
To cite this paper please use the final published version:
DOI: 10.1007/978-3-030-22747-0_46

3 Bi-level approach

3.1 Context and motivation

One of the main limitation experienced by the present hybrid vortex method is related to the computational resources needed to deal with large problems. Indeed, the Eulerian grid used in this work to solve equations 3 to 5 in the splitting algorithm is a uniform Cartesian grid. Therefore, when increasing the Reynolds number in the present direct numerical simulations, the handling of a uniform Cartesian grid requires to consider prohibitive mesh sizes in order to correctly capture the boundary layer, which makes the computation unaffordable. In order to overcome this problem, a good solution relies in multiresolution [1][11] and grid adaptivity [13]. However all these approaches require major modifications in the computational solver. A more straightforward technique may rely in a LES-like model, that is to say in the derivation of a eddy viscosity model.

The aim of LES models based on the filtered Navier-Stokes equations is to estimate the subfilter scale stress tensor τ_{ij}, which is usually modeled by a dissipation term, allowing the energy to cascade from the large scales to the smallest one.

In this work we propose a *bi-level* approach. It consists in solving the vorticity field $\boldsymbol{\omega}$ on a fine grid while the small scales of the related velocity field are filtered so that we only consider the velocity values on a coarse grid, $\overline{\mathbf{u}}$. The main goal of such approach is to reduce the overall computational cost, more specifically the cost dedicated to the resolution of the Poisson equation, and to afford higher Reynolds numbers. In terms of flow physical description on one side and computational cost on the other side, the bi-level simulations can therefore be considered in between DNS and LES.

Previous studies dealing with multi-resolution simulations in the context of remeshed Vortex Methods have already been performed in [6]. However, in that study, the multi-resolution simulations were dedicated to the transport of a passive scalar. In other words, a coarse grid was used to compute the flow quantities, namely the vorticity and velocity fields, while a fine grid was considered to compute the convected passive scalar. An interpolation was performed to exchange the informations between the coarse and the fine grid quantities, but no eddy viscosity model was needed since the different scales concerned non-coupled variables.

In the work proposed here, the bi-level approach is applied to the $\boldsymbol{\omega}$-$\mathbf{u}$ coupled variables involved in the incompressible Navier-Stokes equations, and relies on the use of a eddy viscosity model. In the context of vortex methods, the derivation of such eddy viscosity model can be done in a different way than the LES subgrid-scale models. We give hereafter the main steps of this model derivation, based on the former studies of [3], and we extend it to our 3D algorithm.

ICCS Camera Ready Version 2019
To cite this paper please use the final published version:
DOI: 10.1007/978-3-030-22747-0_46

3.2 An anisotropic artificial viscosity model

When considering purely Lagrangian vortex methods, one obtains an exact weak solution of convection equations. Therefore, the truncation error of these methods only comes from the regularization used to compute the velocity of the particles from the vorticity field [5]. The artificial viscosity model proposed in this work to handle a *bi-level* approach is based on the dissipative mechanisms embedded in this truncation error. In [3], such artificial viscosity model has been derived in the 2D case by cancelling the positive enstrophy budget embedded in the truncation error of the regularized vorticity transport equation. This artifical diffusion model is anisotropic and is given in 2D by :

$$\frac{d\omega_p}{dt} = C\sum_{q\sim p} v_q(\omega_p-\omega_q)\Big\{[\mathbf{u}(\mathbf{x}_p)-\mathbf{u}(\mathbf{x}_q)]\cdot(\mathbf{x}_p-\mathbf{x}_q)g(|\mathbf{x}_p-\mathbf{x}_q|)\Big\}_+ \tag{8}$$

In the present paper, the model is extended to the 3D case :

$$\frac{d\boldsymbol{\omega}_p}{dt} = \boldsymbol{\nabla}\cdot(\boldsymbol{\omega}_p\mathbf{u}_p)+C\Delta^{-4}\sum_{q\sim p} v_q(\boldsymbol{\omega}_p-\boldsymbol{\omega}_q)\Big\{[\mathbf{u}(\mathbf{x}_p)-\mathbf{u}(\mathbf{x}_q)]\cdot(\mathbf{x}_p-\mathbf{x}_q)g(|\mathbf{x}_p-\mathbf{x}_q|)\Big\}_+ \tag{9}$$

where Δ is the regularization size (or filter size in a LES point of view) and where C is a coefficient depending on the nature and the state of the flow. Note that equation 9 allows to cancel the enstrophy production only in directions of antidiffusion, which provides an anisotropic artificial viscosity model.

In a procedural and algorithmic point of view, the use of such anisotropic artificial viscosity model in the present remeshed vortex method implies the replacement of the stretching equation 4 by equation 9, which now gives the following algorithm :

$$\begin{aligned}
\Delta\mathbf{u} &= -\nabla\times\boldsymbol{\omega}\\
\frac{d\boldsymbol{\omega}_p}{dt} &= \boldsymbol{\nabla}\cdot(\boldsymbol{\omega}_p\mathbf{u}_p)\\
&\quad + C\Delta^{-4}\sum_{q\sim p} v_q(\boldsymbol{\omega}_p-\boldsymbol{\omega}_q)\Big\{[\mathbf{u}(\mathbf{x}_p)-\mathbf{u}(\mathbf{x}_q)]\cdot(\mathbf{x}_p-\mathbf{x}_q)g(|\mathbf{x}_p-\mathbf{x}_q|)\Big\}_+\\
\frac{\partial\boldsymbol{\omega}}{\partial t} &= \frac{1}{Re}\Delta\boldsymbol{\omega}\\
\frac{\partial\boldsymbol{\omega}}{\partial t}+(\mathbf{u}\cdot\nabla)\,\boldsymbol{\omega} &= 0\\
\Delta t_{adapt} &= \frac{\mathrm{LCFL}}{\|\nabla\mathbf{u}\|_\infty}
\end{aligned} \tag{10}$$

4 Numerical results

In order to validate the anisotropic artificial viscosity model proposed in this paper, we consider the Taylor-Green vortex benchmark, which is an unbounded

ICCS Camera Ready Version 2019
To cite this paper please use the final published version:
DOI: 10.1007/978-3-030-22747-0_46

periodic flow commonly used to study the capability of a numerical method to handle transition to turbulence.

The Taylor-Green vortex is an analytical periodic solution of incompressible Navier-Stokes equations. It describes the non-linear interaction of multiscales eddies under the influence of vortex stretching and their final decay. It is a classical benchmark used as an initial condition for numerical methods to study flow problems related to transition to turbulence. This bencharmark has already been tested with success in the context of a remeshed vortex method by van Rees et. al [12]. Since this method was different from the present one in the sense of the remeshing procedure (tensorial versus directional approach in our case), we are eager to test the validity of the method proposed in this work.
We consider the flow that evolves in a periodic cubic box of side length $L = 2\pi$ and develops from the following initial condition, which satisfies the divergence-free constraint:

$$\begin{aligned} u_x(\mathbf{x}, t=0) &= \sin(x)\cos(y)\cos(z) \\ u_y(\mathbf{x}, t=0) &= -\cos(x)\sin(y)\cos(z) \\ u_z(\mathbf{x}, t=0) &= 0 \end{aligned} \tag{11}$$

The Reynolds number of the flow is defined by $Re = 1/\nu$. In the present study it is set to $Re = 1600$. At such regime, the minimum number of grid cells per direction is approximatly given by:

$$n_x \approx \frac{l_0}{\eta} = Re^{3/4} \sim 253 \tag{12}$$

where $l_0 = 1$ denotes the integral length scale, that is to say the scale of the largest eddies, and where $\eta = \left(\frac{\nu^3 l_0}{u_0^3}\right)^{\frac{1}{4}}$ corresponds to the Kolmogorov length scale, that is to say the scale of the smallest eddies, with u_0 the caracteristic velocity set to 1. Therefore, according to this estimation, we expect reliable results from a 253^3 total grid resolution.

4.1 DNS results

First of all, we validate the present remeshed vortex method in the case of Direct Numerical Simulations. The results presented in this subsection are obtained from the splitting algorithm described in the first part (eqs. 3-7).

Grid convergence study In the present grid convergence study the simulations are performed on the following uniform Cartesian grids:

$$n_x \times n_y \times n_z = 64^3,\ 128^3,\ 256^3,\ 512^3 \tag{13}$$

The results are analyzed in terms of enstrophy evolution, where the enstrophy is the integral quantity defined as:

$$Z = \frac{1}{L^3}\int_D \boldsymbol{\omega}^2 \, d\mathbf{x} = \nu^{-1}\varepsilon. \tag{14}$$

ICCS Camera Ready Version 2019
To cite this paper please use the final published version:
DOI: 10.1007/978-3-030-22747-0_46

They are compared in Fig. 2 to the convergence study performed by Jammy et. al using an explicit finite difference solver [7]. We can notice that both methods converge with a 256^3 resolution, which corresponds to the minimum number of cells required in the domain to correctly solve the smallest scales, as explained previously. One can also emphasize an interesting feature of the Vortex Methods which relies on the fact that even with unconverged grids (e.g. 64^3), the correct maximum value of enstrophy at $T \approx 9$ is captured by the present method (Fig. 2a), which is not the case with a finite difference based method (Fig. 2b). This result highlights the low numerical diffusion produced by the present method due to the Lagrangian treatment of advection.

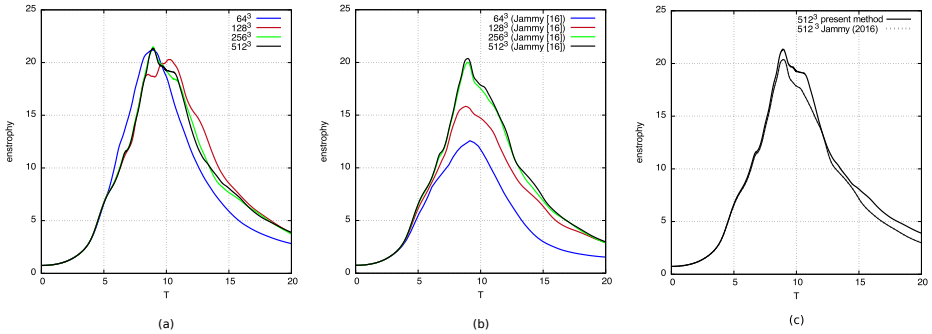

Fig. 2: Grid convergence study in terms of enstrophy evolution. (a) Present method. (b) Results obtained by Jammy et. al [7] with the OpenSBLI solver, based on a finite difference algorithm. (c) Superimposition of the solutions obtained by [7] and the present method with the converged 512^3 resolution.

Validation Based on the results of the previous section, we consider the converged grid $n_x \times n_y \times n_z = 512^3$ for the simulations performed in this validation study. As can be seen on Fig. 2 c), the present solution is in good agreement with the one of [7], especially until $T \approx 9$, when the peak of energy dissipation is reached. A discrepancy between the two results is then observed during the flow mixing stage, showing a slightly more dissipative behavior provided by the present vortex method compared to the finite difference method of [7].

Our results are now qualitatively analyzed in terms of vortical structures in the flow. Fig. 3 shows the norm of vorticity field $|\boldsymbol{\omega}|$ obtained with the present method using a 512^3 resolution in the $x = 0$ plane at $T = 9$, when the maximum of energy dissipation occurs. The vorticity isocontours of the eddy depicted on the close-up view are given below, in Fig. 4, and are compared to the one found in [12] using the same resolution of 512^3. As can be noticed, our results and the one of [12] coincide rather well. A noticeable discrepancy is noticed concerning the shape of the "eye" of the vortical structure. However, the size of the eddy

ICCS Camera Ready Version 2019
To cite this paper please use the final published version:
DOI: 10.1007/978-3-030-22747-0_46

and the thin elongated parts are almost similar for both methods, without any noisy regions.

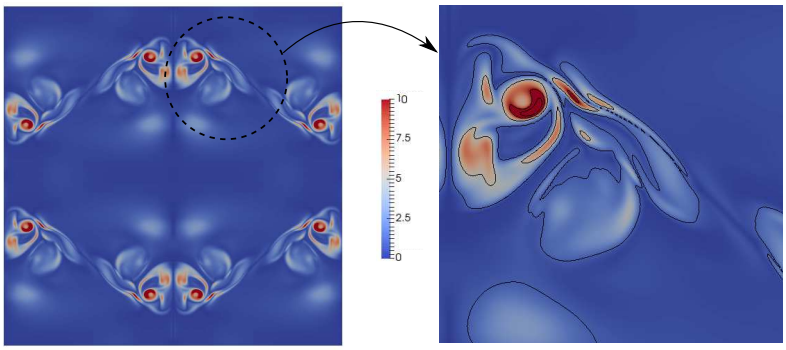

Fig. 3: **T=9.** Instantaneous magnitude of vorticity field $|\boldsymbol{\omega}|$ at $T = 9$ in the $x = 0$ plane with a 512^3 resolution. Global view (left) and close up view (right).

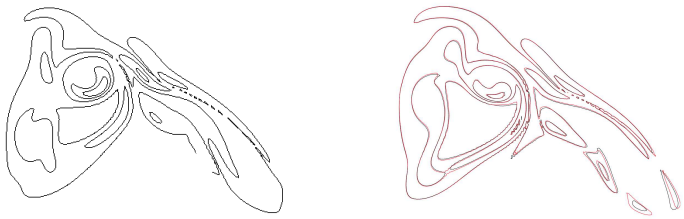

Fig. 4: **T=9.** Instantaneous isocontours of $|\boldsymbol{\omega}|$ for values 1, 5, 10, 20, 30 at $T = 9$ in the $x = 0$ plane with a 512^3 resolution. (Left) Present vortex method. (Right) Results obtained by [12].

4.2 Bi-level results

This section is dedicated to the validation of the anisotropic viscosity model (9) in the context of the Taylor-Green vortex benchmark. The fractional step algorithm used here is the one given in subsection 3.2. As explained previously, the bi-level approach consists in using this artificial viscosity model within the incompressible $(\boldsymbol{\omega}, \mathbf{u})$ Navier-Stokes equations where the vorticity field $\boldsymbol{\omega}$ is solved on a fine grid and where the related velocity field $\mathbf{u}$ is filtered so that we only consider the velocity values on a coarse grid. The velocity filtering is performed

ICCS Camera Ready Version 2019
To cite this paper please use the final published version:
DOI: 10.1007/978-3-030-22747-0_46

through the following cutoff filter, defined in the Fourier space:

$$f_{k_\Delta}(|\mathbf{k}|) = 1 \quad \text{if } |\mathbf{k}| \leq k_\Delta = \frac{\pi}{\Delta} \tag{15}$$

$$0 \quad \text{otherwise} \tag{16}$$

where Δ is the filter size. In the simulations performed below we consider a 64^3 coarse mesh size for the velocity calculations and a 256^3 fine mesh size for the vorticity field. In this case the filter size is therefore equal to $\Delta = 4h$ where h, the fine grid step, is equal to $L/256$.

Fig. 5(a) shows enstrophy evolution curves obtained with model (9) for different values of the constant C. This parametric study on constant C is carried out between $T = 0$ and $T = 10$. This time range is of great importance since it corresponds to the moments when the vortices roll-up and start to interact with each others under the influence of the vortex stretching, leading to the formation of regions of high energy dissipation, until the maximum of dissipation is reached ($T \approx 9$) and kinetic energy is dissipated into heat under the action of molecular viscosity. It emerges from the results given in Fig. 5(a) that the artificial viscosity model (9) set with $C = 0.04$ manages to capture the correct behavior of the flow, especially at the peak of energy dissipation between $T = 8$ and $T = 10$. The enstrophy evolution obtained with $C = 0.04$ is reported in Fig. 5(b) and compared to the DNS result (red and blue solid lines respectively). We also plotted in this figure the curves corresponding to the same simulations where the small scales of the vorticity field have also been filtered only for the evaluation of the enstrophy (denoted "Z" in the figure caption), so that Z is defined on the coarse 64^3 grid (red and blue dashed lines). Fig. 5(b) thus clearly highlights the fact that the model (9), represented by the solid red curve, is between DNS (solid blue curve) and LES (dashed curves) since it allows to take into account the small-scales of the vorticity field.

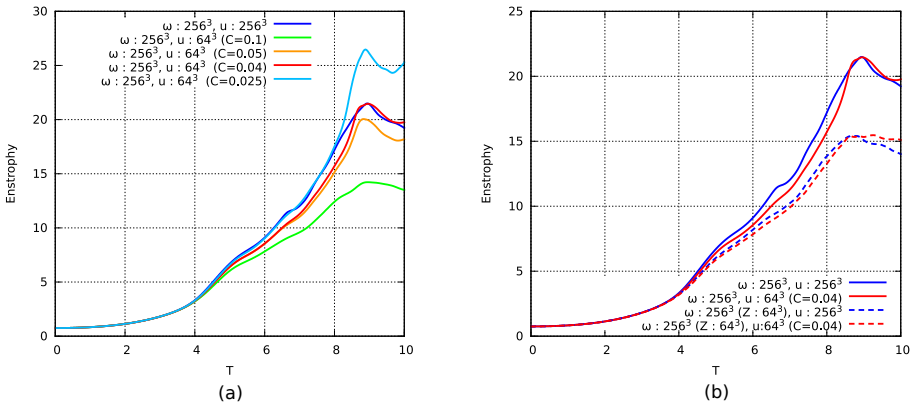

Fig. 5: Enstrophy as a function of time for DNS vs model (9) with (a) different values of C, (b) filtered vorticity values for enstrophy Z evaluation.

ICCS Camera Ready Version 2019
To cite this paper please use the final published version:
DOI: 10.1007/978-3-030-22747-0_46

Simulations based on model (9) were also performed with a $512^3 - 128^3$ bi-level resolution, setting $C = 0.04$. Fig. 6 compares the contours of $|\boldsymbol{\omega}|$ obtained respectively at $T = 8$ and $T = 9$ with a $256^3 - 64^3$ and a $512^3 - 128^3$ bi-level resolution to the contours obtained with DNS based on a 512^3 resolution. These figures show that the contours obtained with model (9) and a $512^3 - 128^3$ resolution are very close in a qualitative point of view to the one given by the Direct Numerical Simulations obtained at 512^3, without spurious vortex structures. These results confirm the capability of the proposed anisotropic artificial viscosity model to adequately resolve the large scales of the flow.

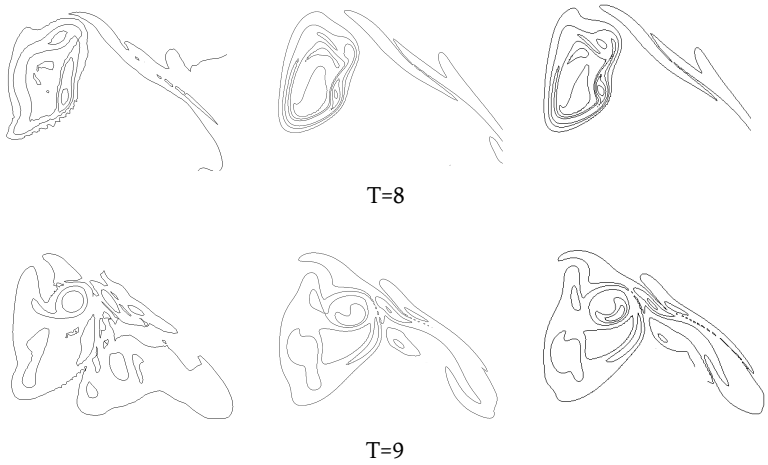

Fig. 6: Contours of $|\boldsymbol{\omega}|$ in the YZ plane at $x = 0$ obtained through the artificial viscosity model (9) ($C = 0.04$) at $T = 8$ and $T = 9$ with a $256^3 - 64^3$ bi-level resolution (left) and a $512^3 - 128^3$ resolution (center). They are compared to the DNS results obtained with a 512^3 resolution (right).

5 Conclusion

In this work, a hybrid vortex method has been employed to simulate a three-dimensional flow. One original feature of this vortex method relies in the remeshing process. The particle advection-redistribution is indeed performed direction by direction, which allows significant computational savings in 3D compared to classical tensorial approaches. The present method has been first validated in the context of Direct Numerical Simulations, showing low numerical diffusion and good agreements with purely grid based high order methods. An anisotropic eddy viscosity model has also been presented in the context of this remeshed vortex method. The results obtained with such model for bi-level simulations

ICCS Camera Ready Version 2019
To cite this paper please use the final published version:
DOI: 10.1007/978-3-030-22747-0_46

constitute an encouraging preliminary study, which has to be tested on other 3D flow types.

Among the next tasks to consider, the main one would consist in dealing with multi-scale problems on hybrid CPU-GPU architecture in order to significantly enhance the computational performances. In practice, we aim to dedicate the high resolution vorticity transport/stretching sub-problems on multi-GPU's while solving the diffusion and Poisson equations on multi-CPU's with a velocity field defined on a coarse grid. This strategy would therefore require interpolation operations between the two coupled flow quantities.

References

1. Bergdorf, M., Cottet, G.H., Koumoutsakos, P.: Multilevel adaptive particle methods for convection-diffusion equations. Multiscale Modeling and Simulation: A SIAM Interdisciplinary Journal **4(1)**, 328–357 (2005)
2. Cocle, R., Bricteux, L., Winckelmans, G.: Scale dependence and asymptotic very high Reynolds number spectral behavior of multiscale subgrid models. Physics of Fluids **21(8)** (2009)
3. Cottet, G.H.: Artificial viscosity models for vortex and particle methods. J. Comput. Phys. **127**, 199–208 (1996)
4. Cottet, G.H., Etancelin, J.M., Perignon, F., Picard, C.: High order semi-lagrangian particles for transport equations: numerical analysis and implementation issues. ESAIM: Mathematical Modelling and Numerical Analysis **48**, 1029–1064 (2014)
5. Cottet, G.H., Koumoutsakos, P.: Vortex Methods - Theory and Practice. Cambridge University Press (2000)
6. Etancelin, J.M.: Couplage de modèles, algorithmes multi-échelles et calcul hybride. Ph.D. thesis, Université de Grenoble (2014)
7. Jammy, S., Jacobs, C., Sandham, N.: Enstrophy and kinetic energy data from 3D Taylor-Green vortex simulations. https://eprints.soton.ac.uk/401892/ (2016)
8. Koumoutsakos, P., Leonard, A.: High-resolution simulations of the flow around an impulsively started cylinder using vortex methods. J. Fluid Mech. **296**, 1–38 (1995)
9. Magni, A., Cottet, G.H.: Accurate, non-oscillatory remeshing schemes for particle methods. J. Comput. Phys. **231(1)**, 152–172 (2012)
10. Mansfield, J., Knio, O., Meneveau, C.: A dynamic LES scheme for the Vorticity Transport Equation: Formulation and a priori tests. J. Comput. Phys. **145**, 693–730 (1998)
11. Rasmussen, J.T., Cottet, G.H., Walther, J.H.: A multiresolution remeshed vortex-in-cell algorithm using patches. J. Comput. Phys. **230**, 6742–6755 (2011)
12. van Rees, W.M., Leonard, A., Pullin, D., Koumoutsakos, P.: A comparison of vortex and pseudo-spectral methods for the simulation of periodic vortical flows at high reynolds numbers. J. Comput. Phys. **230(8)**, 2794–2805 (2011)
13. Rossinelli, D., Hejazialhosseini, B., van Rees, W.M., Gazzola, M., Bergdorf, M., Koumoutsakos, P.: MRAG-I2D: Multi-resolution adapted grids for remeshed vortex methods on multicore architectures. J. Comput. Phys. **288**, 1–18 (2015)

ICCS Camera Ready Version 2019
To cite this paper please use the final published version:
DOI: 10.1007/978-3-030-22747-0_46